Metrol. Meas. Syst., Vol. 32 (2025) No. 3, pp. 1–15
DOI: 10.24425/mms.2025.154673

PAN POLSKA AKADEMIA NAUK

METROLOGY AND MEASUREMENT SYSTEMS
Index 330930, ISSN 0860-8229
www.metrology.wat.edu.pl

M&MS

IMPACT OF STL FILE FORMAT ON THE CYLINDRICITY DEVIATION OF MODELS MANUFACTURED USING FDM TECHNOLOGY

Paweł Zmarzły, Paweł Szczygieł, Anna Bujarska

1) Kielce University of Technology, Faculty of Mechatronics and Mechanical Engineering, Tysiąclecia Państwa Polskiego 7 Ave., 25-314 Kielce, Poland (✉ *pzmarzly@tu.kielce.pl*)

Abstract

Fused Deposition Modelling (FDM) is a category of MEX additive manufacturing processes that has gained considerable popularity. Its ability to produce cylindrical machine parts makes it a particularly useful technology in this field. In order to ascertain the accuracy of the cylindrical component, it is necessary to carry out a measurement and evaluation of the cylindricity deviation. This measurement can identify defects that are the consequence of the 3D printing process, thus providing valuable insight into the quality of the printed object. Nevertheless, in numerous studies, the impact of the manner in which STL digital files are saved on the formation of errors in the shape of cylindrical elements is overlooked. This article presents studies aimed at determining the influence of STL recording of a virtual model on the accuracy of the printout, as determined by the cylindricity deviation. The measurements were conducted using a Prismo Navigator coordinate measuring machine produced by Zeiss. It has been demonstrated that the manner in which a digital file is saved has an effect on the characteristics of irregularities in cylindrical surfaces, which, in turn, affects the value of cylindricity deviation. The findings of the study, as detailed in the article, will provide a framework for the selection of parameters for the recording of STL files, with the objective of obtaining cylindrical surfaces of an acceptable quality, *i.e.* the lowest value of cylindricity deviation.

Keywords: 3D printing, FDM, MEX, cylindricity.

1. Introduction

The use of additive technologies is becoming increasingly prevalent in industrial production based on ISO or ASME standards [1]. The growing prevalence and enhanced characteristics of construction materials have facilitated the integration of 3D printing in a multitude of economic sectors, including the electronics industry and the medical field [2]. In the latter, 3D printing is employed in the fabrication of prostheses, implants, and personal protective equipment [2, 3]. The necessity to reduce costs and produce the highest quality goods requires the parameters of the *stereolithography* or *standard tessellation language* (STL) file to be adjusted in order to ensure the smallest possible shape errors and desired mechanical properties are achieved during the printing process [4]. Additive manufacturing is a method of creating a three-dimensional

Article history: received December 23, 2024; revised February 23, 2025; accepted May 22, 2025; available online July 11, 2025.

object by layering materials according to a digital model created using *computer-aided design* (CAD) software. The PN-EN ISO/ASTM 52900 [5] standard defines various categories of additive manufacturing, including bonding of powdered material with liquid *binder jetting* (BJT), *vat photopolymerization* (VPP) or the most popular layer extrusion of *material extrusion* (MEX). The final category comprises *fused deposition modelling* (FDM), *fused filament fabrication* (FFF), and *layer plastic deposition* (LPD) technologies. The study described in this article will be carried out using FDM technology.

Fused deposition modelling technology was first developed in the late 1980s. Currently, this is the dominant method of 3D printing. The process is most commonly referred to as "3D printing of plastic". The design of the printed model should be done using 3D modelling software CAD programmes. It is a prerequisite that the programme is capable of saving the model in the STL format, whereby the model is represented as a mesh of triangles in a three-dimensional space. In FDM technology, models are constructed using filaments (plastics for formation of diverse geometries by applying elevated temperatures, typically within the range of 190°C to 260°C, in the majority of 3D printers). The print head is positioned in such a way that it moves in an XY plane, with the X-axis representing the movement of the head and the Y-axis representing the movement of the work table. Once the initial layer has been deposited, the worktable is lowered in the Z-axis direction, or alternatively, the head is elevated in the Z-axis direction, allowing the next layer of the 3D model to be applied. The precise action depends on the design of the 3D printer in question. Prior to the application of an additional layer to the pre-existing printed one, it is essential that the latter undergoes a cooling and hardening process. In this manner, a spatial model of the element is constructed in a gradual, additive process. A distinctive feature of this additive technology is the necessity for the utilisation of supports, namely load-bearing structures that are constructed concurrently with the model or support material. It is essential to provide support for any component that features overhangs or is suspended in the air. The use of supports enables the printing of intricate geometric shapes; however, the removal of these supports can be challenging [6, 7]. The authors [6] pointed out that optimising the printing process can result in improved mechanical properties such as tensile strength, fatigue strength, and tribological properties. Optimised 3D printing can be used to develop different surface textures for various friction and wear applications, as well as in robotics applications for gripping.

Digital models saved in the STL format are three-dimensional solids whose surfaces are composed of triangles. The most basic solid that can be described in this way can be considered a tetrahedron, composed of four triangles, each of which is also a whole wall. An alternative model is that of a cuboid, in which each of the rectangular walls is constructed from two triangles. In this article, the shape of the test model is taken from ISO/ASTM 52902 [8]. This standard provides a general description of the geometry of reference samples used to assess the accuracy of manufacturing elements using selected 3D printers. The present standard does not provide detailed specifications regarding the measurement parameters and sampling strategies. This applies both to contact and optical methods [9, 10].

The objective of the research presented in this article is to analyse the impact of the STL digital file on the value of shape errors, as represented by the cylindricity deviation of the 3D printed models. There are a lot of methods used to measure roundness and cylindricity [11, 12]. It should be noted that excessive values of cylindricity deviation have the potential to cause vibrations in elements that are subjected to rotational movement, or to result in assembly issues, such as those observed in screw joints [13]. The analysis of shape errors is the subject of a substantial body of research [14, 15]. Work [14] contains a detailed analysis of cylindrical elements by measuring cylindricity and surface roughness. It has been demonstrated that measurement parameters have a significant impact on the values of the surface roughness and cylindricity parameters. The authors of [15] investigated the

dimensional accuracy and quality of the surface layer of parts produced by 3D printing. The findings indicated that the orientation of the print has a significant impact on the quality of the finished product. In work [16], the authors examined the possibility of using direct metal laser melting technology to produce cutting tools, namely drills. The quality of holes drilled in polyamide PA6 was evaluated using a printed drill, taking into account the variable cutting parameters. The shape of the holes was analysed in terms of their roundness, cylindricity, and straightness. It has been demonstrated that *direct metal laser melting* (DMLM) technology can be effectively employed for the fabrication of prototype drills. The subject raised in article [17] concerns the assessment of errors in the shape of the crankshafts of a large marine engine using measuring systems used directly in industrial conditions. It has been demonstrated that the choice of the support method has a significant impact on the accuracy of measurements taken of large cylindrical objects.

The *Standard Tessellation Language* (STL) file has undoubtedly become the rapid prototyping standard. The file is made up of a series of connected triangles that describe the surface geometry of an object or a 3D model. As a result, the more complex the design, the more triangles are used and the higher the resolution. This also has the effect of a greater load on the software memory used for mesh generation. The representation of the 3D solid is a triangular mesh generated by tessellation of its boundary surface. In engineering applications, this mesh needs to contain information about which side of the triangle is on the inside of the solid. The STL file is therefore a representation of the triangular surface in which the vertices of each triangle are ordered to fulfil this requirement [18]. ISO/ASTM 52950 *additive manufacturing – General principles – Overview of data processing* [19] specifies the recording formats used in 3D printing technology STL is the most commonly used format for transferring data. It is a system-neutral format for the exchange of pure geometric data. It uses triangles and their normal vectors to describe the boundary surfaces of volumetric models.

In the literature, one can find studies on the identification and analysis of common errors [20] that can occur when working with files of this format and defining key criteria for assessing the geometric quality of the mesh. Studies to modify triangle meshes to optimise print quality have been carried out in subsequent publications [18, 21, 22]. The paper [18] presents a method for detecting defects in surface mapping by building a multiwall data structure from an STL file. However, in [21], a surface-based modification algorithm is presented, which, adaptively and locally, increases the density of the STL model's facets. The Surface-based Modification Algorithm is an error minimising approach to locally modify the STL mesh based on chord error, cusp height, and cylinder error for cylindrical features and is typically able to achieve a smaller file size compared to the Unified Export option. The aim of the method proposed [22] is to show the possibility of generating adaptive surface meshes suitable for the finite element method, directly from an approximate boundary representation of an object created with CAD proving that not using the parametric representation of the geometric model allows to override some of the limitations of conventional meshing software that is based on an representation of the geometry.

In most research papers, the authors focus on assessing the influence of technological parameters, type of material, and postprocessing on the quality of manufactured parts. In connection with the emergence of new guidelines contained in [8], which concern the method of 3D printing and measurement of selected geometric features, the paper assesses the impact of digital file recording on the value of cylindricity deviation of cylindrical elements. In [23] it was pointed out that changing the STL mesh shaping algorithm or modifying it afterward can have a beneficial effect on the quality of 3D printing.

The studies presented in this article provide guidelines for the selection of parameters for recording an STL file in order to obtain cylindrical elements with the least cylindricity deviation. In addition, a recommended strategy for measuring this type of shape deviation is indicated.

2. Materials and Methods

The research procedure consisted of several steps. It started with designing samples in selected CAD software. At this stage, digital 3D models were created and then exported to the STL format for further processing in 3D printing technology. The next step involved importing STL files into 3D printer software and manufacturing samples using 3D printing. Once printed, the samples were subjected to cylindricity measurements. Subsequently, the samples were subjected to macroscopic observations to assess their surface quality and detect potential surface defects. The flow chart of the research procedure is presented in Fig. 1.

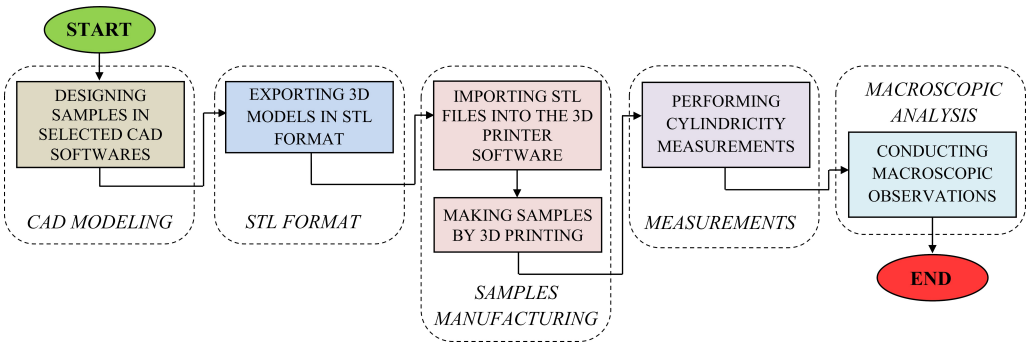

Fig. 1. Flow chart of the research procedure.

2.1. Materials

The material used in the study was *polylactic acid* (PLA) with a density of 1.24 g/cm^3 in the form of a 1.75 mm diameter filament with the trade name Fiberlogy easy PLA (*Fiberlab*, Brzezie, Poland). Table 1 shows its selected mechanical properties.

Table 1. Selected mechanical properties [24].

Mechanical properties	Test Method	Unit	Value
σ_y	ISO 527	MPa	50
σ_b	ISO 527	MPa	53
E	ISO 527	MPa	3500
ε_y	ISO 527	%	6
σ_f	ISO 178	MPa	81
E_f	ISO 178	MPa	3800

2.2. Research model

The samples were designed in accordance with [8] in *SOLIDWORKS* (Dassault Systèmes, Vélizy-Villacoublay, France) and in *Siemens NX* (Siemens, Munich, Germany). The programmes use from their own algorithms to convert the model to the STL format. In this article, the STL mesh arrangement in *SOLIDWORKS* programme is referred to as Method 1, while the STL mesh arrangement in *Siemens NX* programme is designated as Method 2.

Most CAD software environments allow the 3D model to be saved in the STL save format, with controlled deviation and angle parameters, for example *FreeCAD*, Fusion [25, 26]. However, it should be noted that these programs can perform the triangulation operation with different algorithms. In addition, *SOLIDWORKS* and *Siemens NX* are the programmes most commonly used in the industrial environment, so this approach seems appropriate in practical terms. In the future, it is planned to extend the research to other software with triangulation algorithms different from those presented in this article.

Figure 2 shows the geometry of the sample, consisting of two concentric rings that are closely spaced together. The concentric rings are centred on a thin circular plate. A *medium* variant sample was used.

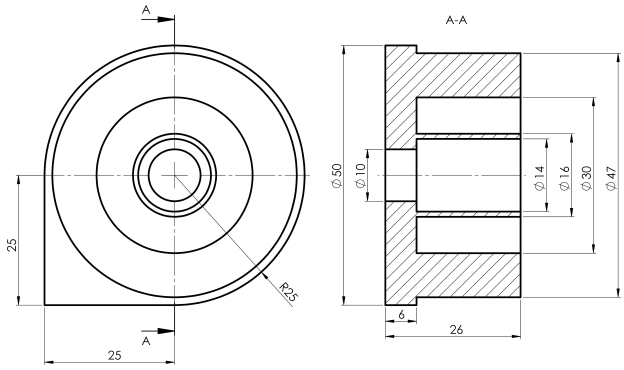

Fig. 2. Medium sample dimensions [8].

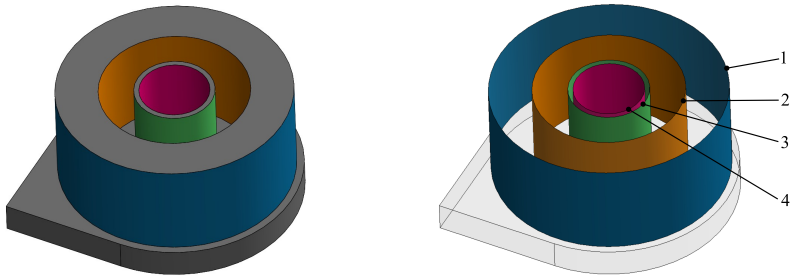

Fig. 3. View of the CAD model: (A) full; (b) excluding the top surface to show the measured surface, where: 1 – Surface 1, 2 – Surface 2, 3 – Surface 3, 4 – Surface 4.

The samples were saved in the STL format (with the surface described using triangles). The mesh parameters are included in Table 2.

Table 2. Mesh parameters.

Method	**Deviation Tolerance, mm**	**Angle Tolerance, °**	**Number of triangles**
1	±0.01	±1	8288
2	±0.01	±1	8288

Figure 4 shows the mesh views of the models in which Figs. 4a and 4b represent the meshes obtained successively by Method 1 and Method 2, while Fig. 4c shows the differences resulting from the mesh arrangement for Methods 1 and 2.

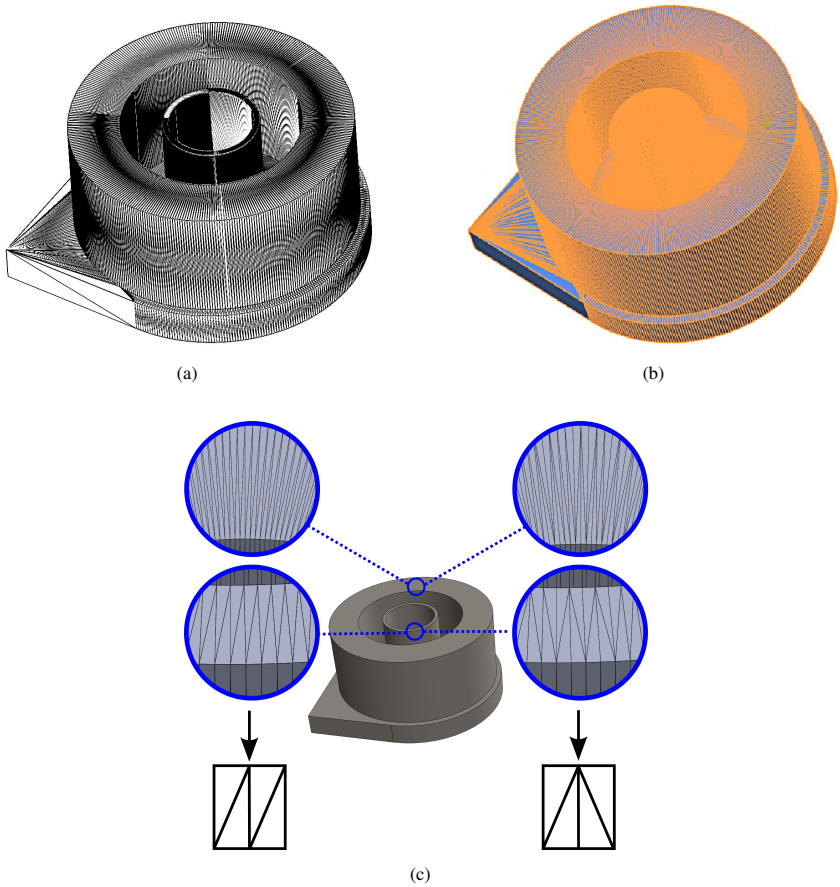

Fig. 4. STL mesh: a) obtained using Method 1, b) obtained using Method 2, c) comparison of the methods.

On the basis of the mesh view in Fig. 4, another way can be observed in which the methods under analysis can be interlinked. In Method 1, the individual facets resemble rectangular triangles, while in Method 2, the facets resemble isosceles triangles. It should be added that there is a difference in the density of the triangles depending on the selected surface, which can have an effect on the quality of the print surface.

2.3. 3D printing technology

In order to produce the samples, the FDM/FFF 3D printing technology, which falls into the category of MEX according to [5], was used. This technology involves extruding a thermoplastic material through a heated nozzle. The material in a semi-liquid state is applied to the printer's work table (bed), and a 3D model is then built layer by layer. A 3D MakerBot Sketch printer

(*MakerBot*, USA, New York) was used. According to the manufacturer, the chemical composition of the material is > 98% polyactide plus filler and functional additives [27]. The 3D printing parameters are included in Table 3.

Table 3. 3D printing parameters.

Parameter	Unit	Value
Extruder temperature	°C	220
Bed temperature	°C	65
Shell	–	2
Layer Height	Mm	0.1
Printing pattern	–	Linear
Infill density	%	50

Based on the digital STL models obtained by Methods 1 and 2, a number of samples were produced for measurements. Two series of samples were used for the study. One was produced using Method 1 and the other using Method 2, with each series consisting of 10 samples, thus a total of 20 samples were produced. However, the results of the measurements presented should be regarded as statistical values from the series of measurements. Photographs of printed samples are shown in Fig. 5.

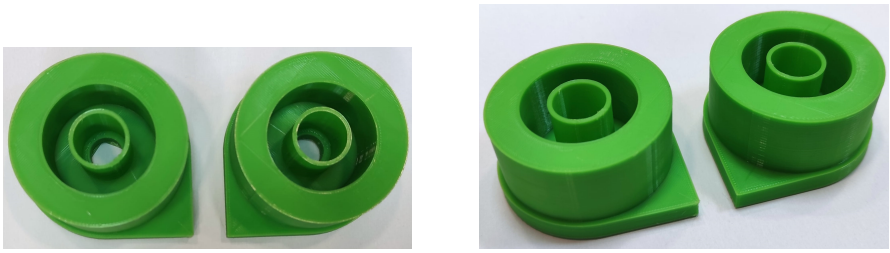

(a) (b)

Fig. 5. Photographs of the actual models: a) Method 1, b) Method 2.

2.4. Measurement of cylindricity

According to PN-EN ISO 1101:2017-05, cylindricity deviation (ΔC) is the largest distance between points on the actual surface and the surface of the reference cylinder that is tangential to the area of the partial zone. A reference cylinder is one with the smallest diameter inscribed on the surface of the shaft or the one with the largest diameter circumscribed to the surface of the hole. The boundary of the tolerance zone is formed by two coaxial cylinders with radii differing by a value t from the specified allowed tolerance for this deviation. Previous practice has shown that the most straightforward cylinder to define is the associated cylinder determined using the least squares method. The parameter determined relative to this cylinder is defined as CYL_t. It is the sum of the largest positive absolute value and the largest negative local cylindricity deviation, both measured relative to the associated cylinder determined by the least squares method, as defined by the formula:

$$CYL_t = CYL_p + CYL_v, \tag{1}$$

where: CYL_p the value of the largest positive local cylindricity deviation measured relative to the reference cylinder, which is determined using the least squares method; CYL_v the absolute value of the largest negative local cylindricity deviation relative to the reference cylinder, also determined using the least squares method.

Active or passive scanning probe heads are used to carry out specialised measurements with the *coordinate measuring machine* (CMM). In the case of using impulse heads, the measurement time and selection of the optimal number of measuring points become a problem, because the adopted number of points will depend, among others, on the error in assessing the cylindricity profile [29]. As a result, the study uses a Zeiss VAST Gold scanning head (Zeiss, Oberkochen, Germany), which enables scanning at different speeds even at very high values (up to 300 mm/s) thanks to the use of the Navigator system. The accuracy of form error measurement in the CMM is increased by the use of active scanning heads. To assess the cylindricity deviation of precision machine parts, $e.g.$ rolling bearing components, it is recommended to use specialised measuring systems based on the method of measuring radius changes. Due to the relatively large values of the cylindricity deviations of parts made using additive MEX technologies, the use of a coordinate measuring technique for such an assessment is sufficient.

The *Zeiss Prismo Navigator* coordinate measuring machine and *Zeiss Calypso* software (*Zeiss*, Oberkochen, Germany) were used for the measurements. The measurements were carried out under controlled conditions at an ambient temperature of 20°C. The parameters listed in Table 4 characterise the selected measuring machine.

Table 4. Parameters of the coordinate measuring machine.

Parameter	Value
Measurement range	X = 900 mm; Y = 1200 mm, Z = 700 mm
Max. permissible error/spindle error	0.9 + (L / 350) µm

The measurements were carried out using precision styli with 3 mm diameter ruby spheres, $i.e.$ ones with the smallest possible diameter, which was due to the nature of the irregularities occurring on the surface of the elements to be measured, in order to reduce the possibility of mechanical filtration. The sampling step size was 0.05 mm. Two measurement speeds were used, depending on the diameter dimension of the sample surface. Surfaces 1 and 2 (Fig. 3b) were measured at 10 mm/s. Surfaces 3 and 4 were measured at 5 mm/s. Because of the values of the cylindricity deviation, these are typical stylus feed rates when measuring form deviations on a CMM.

In this research, the probe was not qualified by the dynamic tensor method, so in order to maintain the same sampling level for all surfaces, it was necessary to reduce the scanning speed for smaller diameters.

3. Results

In order to determine the cylindricity deviation, the measured profiles were filtered with a Gaussian filter in the range of 2-50 UPR, which allows analysis of the waviness components in addition to the shape error. The deviation was determined on the basis of the reference cylinder, the so-called medium cylinder, determined by the least squares method. The results of the measurements of the cylindricity parameter are presented in Table 5 and Fig. 6, where the surfaces correspond to those indicated in Fig. 3b, while the values obtained characterise the parameter CYL_t.

Metrol. Meas. Syst., Vol. 32 (2025), No. 3, pp. 1–15
DOI: 10.24425/mms.2025.154673

Table 5. Measurement results.

Surface No.	Method 1		Method 2	
	$\overline{x}$ mm	SD, mm	$\overline{x}$ mm	SD, mm
1	0.1792	0.0330	0.2475	0.0485
2	0.1425	0.0126	0.1847	0.0212
3	0.1353	0.0401	0.1820	0.0374
4	0.1142	0.0234	0.1915	0.0188

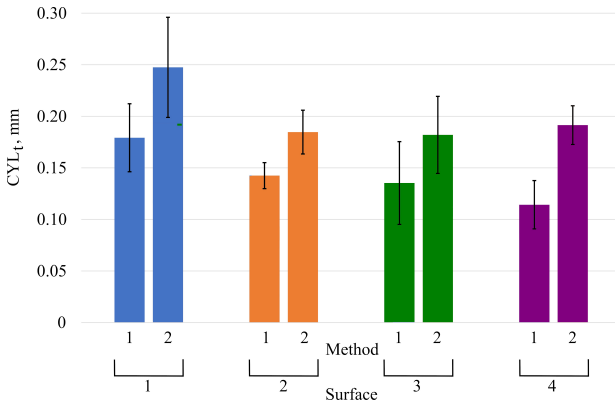

Fig. 6. Measurement results.

In order to evaluate the nature of surface irregularities of cylindrical surfaces, Figs. 7 and 8 present the profiles of cylindricity for individual surfaces of selected samples manufactured using FDM technology, based on digital files saved using both Method 1 and Method 2.

In assessing the cylindricity character of the measured surfaces shown in Fig. 7 (digital files recorded using Method 1), the presence of ovality was noted, particularly on the outer surface of the model with the largest diameter (Fig. 3a and Fig. 7a). However, when assessing the results of the cylindricity profile measured on the samples produced from the digital file recorded by Method 2 (Fig. 8), a clear conicity can be observed in addition to ovality. In both recording Methods 1 and 2, ovality may be the result of the formation of the so-called "seam", which is related to the initial location of the overlap of individual layers of material. On the other hand, the visible conicity

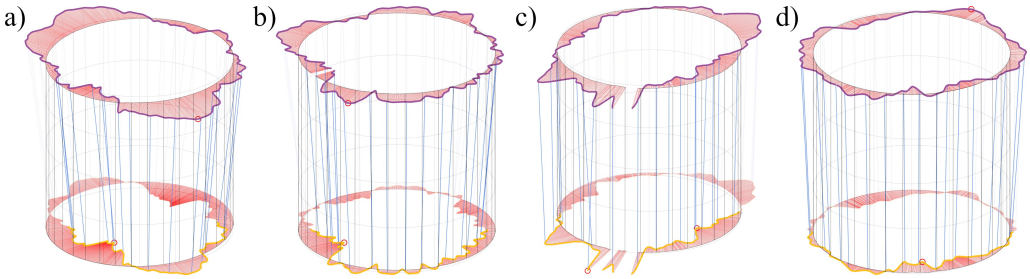

Fig. 7. Cylindricity profiles of the surface of samples manufactured using Method 1: a) Surface 1, b) Surface 2, c) Surface 3, d) Surface 4.

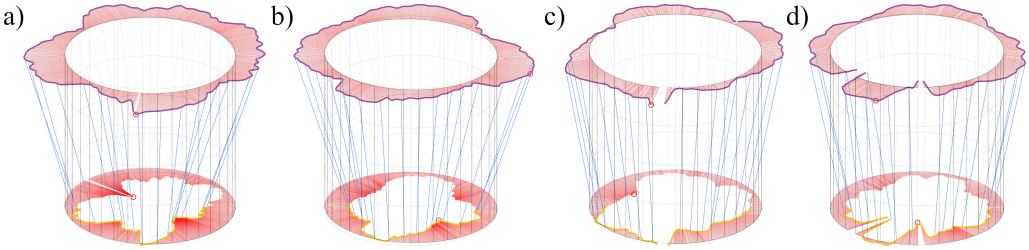

Fig. 8. Cylindricity profiles of the surface of samples manufactured using Method 2: a) Surface 1, b) Surface 2, c) Surface 3, d) Surface 4.

can result from a specific way of bonding and cooling each layer of the material. There may be "blending" of the layers on the outer surfaces, which can be seen as an increase in the model's diameter with each successive layer being applied. It should be noted that for Method 2, higher cylindricity deviation values were recorded for all examined surfaces.

In order to better illustrate the characteristics resulting from the digital STL file format, additional microscopic measurements were made using a MAHR vision MN320 (*Mahr*, Göttingen, Germany) digital microscope, with an optical magnification of X1 and reflected light. Views of the measured surfaces are shown in Fig. 9, where the outline of the STL file is additionally marked.

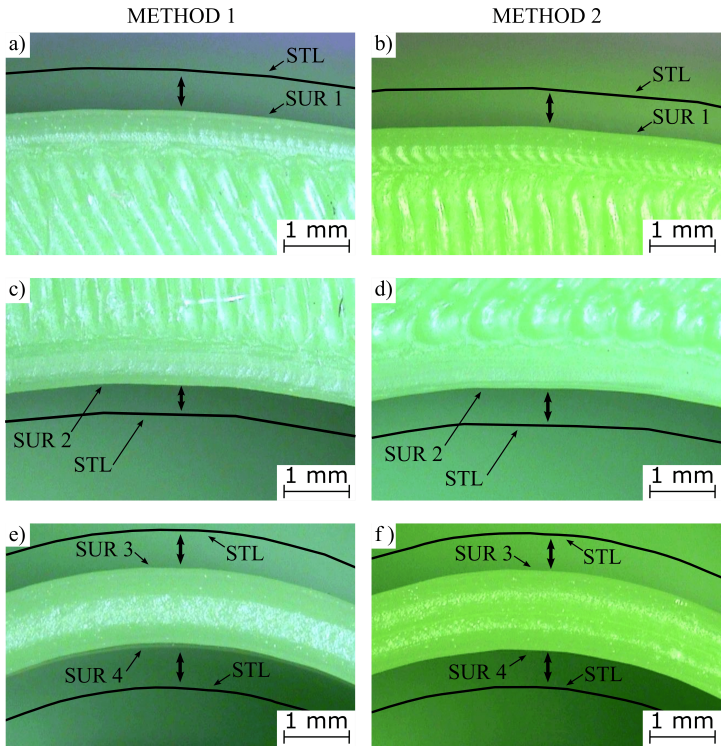

Fig. 9. Macroscopic view of the outline of the sample surfaces: a) Method 1, Surface 1; b) Method 2, Surface 1; c) Method 1, Surface 2; d) Method 2, Surface 2; e) Method 1, Surfaces 3 and 4; f) Method 2, Surfaces 3 and 4.

Analysing the macroscopic views shown in Fig. 9, it is possible to see the visible traces of the individual layers of material applied, together with their directionality. In Method 1, the individual layers of material are similar in shape to rectangular triangles, while in Method 2 they are similar to an isosceles triangle. This is in line with the nature of the triangle mesh in Fig. 4. In addition, Surface 1 in particular shows the refraction of cylindrical profiles. These are similar to the irregularities of the saved digital STL file. Both samples made from digital files recorded using Method 1 and Method 2 show this phenomenon.

3.1. Discussion

In the article [30] the effect of the diameter of the printing nozzle on cylindricity deviation was investigated. The results showed that the smallest cylindricity deviation was obtained for a nozzle size of 0.4 mm and its average value was 0.0700 mm, with a printed piece diameter of 10 mm. In that paper, such a diameter of the printing nozzle was also used and the smallest value obtained was 0.1142 mm, for a diameter of 14 mm. This confirms the relationship that the smaller the diameter of the component, the smaller the cylindricity.

Wolf *et al* [31] checked the effect of different printer drive systems on cylindricity deviation. The tested cylinder had a diameter of 7.5 mm and was made of PLA material, and the average value of the cylindricity deviation was (for the stepper motor) 0.1055 mm. The 3D printer used for the research in this article is also equipped with a stepper motor. This again confirms that the diameter of the part has a direct effect on the cylindricity deviation.

4. Conclusions

3D printing is becoming more widespread as additive manufacturing technologies continue to develop. Initially, 3D printing was only used to create mock-ups and prototypes. These were used to give a visual representation of the final product. Today, fully functional machine parts can be produced using additive technologies. Therefore, one should look out for procedures aimed at increasing the accuracy of the elements produced by means of 3D printing. Most of the research work is focused on the evaluation of types of building materials or technological parameters describing the accuracy of prints or their mechanical properties. However, there is a limited amount of research on the influence of the parameters used to capture the digital STL file on the quality of the printed elements. This is important because saving a digital file is the first step in the printing process. This article assesses the impact of digital STL file storage methods on the quality of cylindrical surfaces using the two most popular CAD software.

Analysis of the results allows one to draw the following conclusions:

1. The results of the research presented in the article showed the visible effect of the way in which the STL file was stored on the cylindricity deviation values. The meshes of the STL model were created differently depending on the method of saving the file. In Method 1 the rectangular triangles were dominant, whereas in Method 2 the equilateral triangles were dominant (Fig. 4).
2. Microscopic analysis of the models showed that the way the triangle mesh was stored in the STL file was replicated in real models (Fig. 9).
3. The cylindricity profiles were characteristic curves (Figs. 7 and 8). In addition, the *CYLt* cylindricity deviation itself depended on the type of digital file storage method. The difference was greater than 40% in some surfaces (Fig. 6).

4. For both methods of saving the STL file, it was observed that with an increase in the diameter of the printed cylindrical surfaces, the value of the *CYLt* cylindricity deviation increased. For Method 1, the difference between the mean value of the cylindricity deviation of the Surface 1 (with the largest diameter) and the Surface 4 (with the smallest diameter) was about 57%. And for Method 2, the difference was approximately 29%.
5. When the contours of the cylindricity stock were evaluated, ovality and conicity were found to be present, which is a direct result of the way the layers are combined in FDM technology. Research has shown that the use of scanning CMM probes can detect defects resulting from the process of combining individual layers of material in FDM technology (Figs. 7 and 8).
6. Taking the smallest cylindricity deviation values as a criterion, Method 1 should be selected.

As a direction for further research, the authors will assess the impact of digital file recording in other additive technologies, such as PolyJet Matrix or Selective Laser Sintering. We also would like to evaluate other geometric deviations, such as flatness. In addition, work is being carried out on the optimisation of a triangle mesh in order to have models with minimal shape deviations.

5. Appendices

Table 6. Nomenclature.

Nomenclature	Description
σ_y	Tensile Strength at Yield
σ_b	Tensile Strength at Break
E	Tensile Modulus
ε_y	Extension at Yield
σ_f	Flexural Strength
E_f	Flexural Modulus
FDM	Fused Deposition Modelling
MEX	Material Extrusion
STL	Standard Tessellation Language
CAD	Computer Aided Design
FFF	Fused Filament Fabrication
ΔC	Cylindricity deviation
CYL_t	Sum of the largest positive absolute value and the largest negative local cylindricity deviation, both measured relative to the associated cylinder determined by the least squares method
CYL_p	Value of the largest positive local cylindricity deviation measured relative to the reference cylinder, which is determined using the least squares method
CYL_v	Absolute value of the largest negative local cylindricity deviation relative to the reference cylinder, also determined using the least squares method
CMM	Coordinate Measuring Machine
$\overline{x}$	Mean
SD	Standard Deviation

References

[1] Humienny, Z., & Zdrojewski, P. (2023). ISO GPS and ASME GDT standards – differences and similarities in definitions of measurands. *Metrology and Measurement Systems*, 30 (4), 791–808. https://doi.org/10.24425/mms.2023.147954

[2] Espera, A. H., Dizon, J. R. C., Chen, Q., & Advincula, R. C. (2019). 3D-printing and advanced manufacturing for electronics. *Progress in Additive Manufacturing*, *4*(3), 245–267. https://doi.org/10.1007/s40964-019-00077-7

[3] Advincula, R. C., Dizon, J. R. C., Chen, Q., Niu, I., Chung, J., Kilpatrick, L., & Newman, R. (2020). Additive manufacturing for COVID-19: Devices, materials, prospects, and challenges. *MRS Communications*, *10*(3), 413–427. https://doi.org/10.1557/mrc.2020.57

[4] Petruse, R. E., Simion, C., & Bondrea, I. (2024). Geometrical and dimensional deviations of Fused Deposition Modelling (FDM) Additive-Manufactured Parts. *Metrology*, *4*(3), 411–429. https://doi.org/10.3390/metrology4030025

[5] PN-EN ISO/ASTM 52900:2022-05. (2022). Additive manufacturing – General principles – Fundamentals and vocabulary.

[6] Shahrubudin, N., Lee, T., & Ramlan, R. (2019). An overview on 3D printing technology: technological, materials, and applications. *Procedia Manufacturing*, *35*, 1286–1296. https://doi.org/10.1016/j.promfg.2019.06.089

[7] Rouf, S., Raina, A., Haq, M. I. U., Naveed, N., Jeganmohan, S., & Kichloo, A. F. (2022). 3D printed parts and mechanical properties: Influencing parameters, sustainability aspects, global market scenario, challenges and applications. *Advanced Industrial and Engineering Polymer Research*, *5*(3), 143–158. https://doi.org/10.1016/j.aiepr.2022.02.001

[8] PN-EN ISO/ASTM 52902:2024-01. (2024). Additive manufacturing – Reference samples – Assessment of geometric accuracy of additive manufacturing systems.

[9] Nowakowski, M., Kurylo, J., & Dang, P. H. (2024). Camera Based AI Models Used with LiDAR Data for Improvement of Detected Object Parameters. In *Lecture Notes in Computer Science* (pp. 287–301). https://doi.org/10.1007/978-3-031-71397-2_18

[10] Gogolewski, D. (2022). Multiscale assessment of additively manufactured free-form surfaces. *Metrology and Measurement Systems*, 30 (1), 157–168. https://doi.org/10.24425/mms.2023.144393

[11] Jermak, C. J., & Rucki, M. (2016). Static characteristics of air gauges applied in the roundness assessment. *Metrology and Measurement Systems*, 23 (1), 85–96. https://doi.org/10.1515/mms-2016-0009

[12] Poniatowska, M., & Werner, A. (2010). Fitting spatial models of geometric deviations of free-form surfaces determined in coordinate measurements. *Metrology and Measurement Systems*, 17 (4), 599–610. https://doi.org/10.2478/v10178-010-0049-x

[13] Grzejda, R. (2016). Modelling nonlinear preloaded multi-bolted systems on the operational state. *Engineering Transactions*, *64*(4), 525–531. https://doi.org/10.24423/engtrans.738.2016

[14] Zaborski, A., & Winczek, J. (2020). Imaging and computer analysis in the shape error measurements and in the cylindrical objects stereometry. *IOP Conference Series Materials Science and Engineering*, *776*(1), 012077. https://doi.org/10.1088/1757-899x/776/1/012077

[15] Chand, R., Sharma, V. S., Trehan, R., Gupta, M. K., & Sarikaya, M. (2022). Investigating the dimensional accuracy and surface roughness for 3D printed parts using a multi-jet printer. *Journal of Materials Engineering and Performance*, *32*(3), 1145–1159. https://doi.org/10.1007/s11665-022-07153-0

[16] Nowakowski, L., Skrzyniarz, M., Blasiak, S., Rolek, J., Vasileva, D., & Avramova, T. (2023). Analyzing the potential of drill bits 3D printed using the direct metal laser melting (DMLM) technology to drill holes in polyamide 6 (PA6). *Materials*, *16*(8), 3035. https://doi.org/10.3390/ma16083035

[17] Nozdrzykowski, K., Grządziel, Z., Grzejda, R., & Stępień, M. (2023). Determination of Geometrical Deviations of Large-Size Crankshafts with Limited Detection Possibilities Resulting from the Assumed Measuring Conditions. *Energies*, *16*(11), 4463. https://doi.org/10.3390/en16114463

[18] Szilvśi-Nagy, M., & Mátyási, G. (2003). Analysis of STL files. *Mathematical and Computer Modelling*, *38*(7–9), 945–960. https://doi.org/10.1016/s0895-7177(03)90079-3

[19] PN-EN ISO/ASTM 52950:2021-07. (2021). Additive manufacturing – General principles – Overview of data processing

[20] Husiev, O., & Nikiforova, T. (2022). Research of the converting stages for the volume model of the product into the control code for a 3D printer in the context of automated construction of 3D printing technology. *Ukrainian Journal of Civil Engineering and Architecture*, *4*, 38–45. https://doi.org/10.30838/j.bpsacea.2312.250822.38.876

[21] Zha, W., & Anand, S. (2015). Geometric approaches to input file modification for part quality improvement in additive manufacturing. *Journal of Manufacturing Processes*, *20*, 465–477. https://doi.org/10.1016/j.jmapro.2015.06.021

[22] Béchet, E., Cuilliere, J., & Trochu, F. (2002). Generation of a finite element MESH from stereolithography (STL) files. *Computer-Aided Design*, *34*(1), 1–17. https://doi.org/10.1016/s0010-4485(00)00146-9

[23] Ledalla, S. R. K., Tirupathi, B., & Sriram, V. (2016). Performance evaluation of various STL file mesh refining algorithms applied for FDM-RP process. *Journal of the Institution of Engineers (India): Series C*, *99*(3), 339–346. https://doi.org/10.1007/s40032-016-0303-4

[24] Fiberlab S.A. (2022). Technical data sheet – Easy PLA. https://fiberlogy.com/wp-content/uploads/2021/12/FIBERLOGY_EASY_PLA_TDS.pdf (access 16.12.2024)

[25] FreeCAD. Import from STL or OBJ. https://wiki.freecad.org/Import_from_STL_or_OBJ (access 19.02.2025)

[26] Autodesk Inc.. How to export an STL/3MF file from Fusion. https://www.autodesk.com/support/technical/article/caas/sfdcarticles/sfdcarticles/How-to-export-an-STL-file-from-Fusion-360.html (access 19.02.2025)

[27] Fiberlab S.A. (2023). Material safety data sheet – Easy PLA. https://fiberlogy.com/wp-content/uploads/v2024/06/FIBERLOGY_MSDS_EASY_PLA.pdf (access 18.02.025)

[28] PN-EN ISO 1101:2017-05. (2017). Geometrical product specifications (GPS) – Geometrical tolerancing – Tolerances of form, orientation, location and run-out

[29] Yang, Y., Wang, T., Chang, Y., Zhang, W., & Cao, M. (2024). Evaluation of Uncertainty in Cylindricity Measurement based on Coordinate Measuring Machine. *Highlights in Science Engineering and Technology*, *107*, 250–253. https://doi.org/10.54097/hdswsh52

[30] Petruse, R. E., Simion, C., & Bondrea, I. (2024). Geometrical and dimensional deviations of Fused Deposition Modelling (FDM) Additive-Manufactured Parts. *Metrology*, *4*(3), 411–429. https://doi.org/10.3390/metrology4030025

[31] Wolf, J., Werkle, K. T., & Möhring, H. (2024). Study on Dynamic Behaviour in FFF 3D-printing with Crossed Gantry Kinematic. *Procedia CIRP*, *121*, 162–167. https://doi.org/10.1016/j.procir.2023.09.244

Paweł Zmarzły received his Ph.D. and D.Sc. from Kielce University of Technology in 2014 and 2022. He is an Associate Professor and Head of the Metrology Laboratory in the Faculty of Mechatronics and Mechanical Engineering at the Kielce University of Technology. He has authored or co-authored 29 JCR publications and 21 patents and utility model patents. His research activities focus on the metrology of geometrical quantities and manufacturing engineering.

Anna Bujarska received her M.Sc. in engineering from the Faculty of Computer Management and Modelling of the Kielce University of Technology. Currently, she is a student of the Doctoral School of the same university in the field of scientific mechanical engineering.

Paweł Szczygieł obtained his B.Sc. and M.Sc. degrees in mechanical engineering from the Kielce University of Technology in 2020. He is currently a research and teaching assistant at the Kielce University of Technology. His research interests focus on the broad applications of 3D printing in medicine.